Original Article

Comparing the outcomes of MR-based versus CT-based tumor delineation in locally advanced non-small cell lung cancer treated with hypo-fractionated radiotherapy and concurrent chemotherapy

Pengxin Zhang[1#]^, Shouliang Ding[1#], Kangqiang Peng[2#], Haoqiang He[2], Daquan Wang[1], Rui Zhou[1], Bin Wang[1], Jinyu Guo[1], Hongdong Liu[1], Xiaoyan Huang[1], Chuanmiao Xie[2], Hui Liu[1], Bo Qiu[1]

[1]Department of Radiation Oncology, State Key Laboratory of Oncology in South China, Collaborative Innovation Center for Cancer Medicine, Guangdong Provincial Clinical Research Center for Cancer, Sun Yat-sen University Cancer Center, Guangzhou, China; [2]Department of Medical Imaging, State Key Laboratory of Oncology in South China, Collaborative Innovation Center for Cancer Medicine, Guangdong Provincial Clinical Research Center for Cancer, Sun Yat-sen University Cancer Center, Guangzhou, China

Contributions: (I) Conception and design: Hui Liu, B Qiu; (II) Administrative support: Hui Liu, B Qiu; (III) Provision of study materials or patients: Hui Liu, B Qiu; (IV) Collection and assembly of data: H He, B Wang, J Guo, Hongdong Liu, X Huang, C Xie; (V) Data analysis and interpretation: P Zhang, S Ding, D Wang, R Zhou; (VI) Manuscript writing: All authors; (VII) Final approval of manuscript: All authors.

[#]These authors contributed equally to this work.

Correspondence to: Bo Qiu, MD, PhD. Department of Radiation Oncology, State Key Laboratory of Oncology in South China, Collaborative Innovation Center for Cancer Medicine, Guangdong Provincial Clinical Research Center for Cancer, Sun Yat-sen University Cancer Center, 651 Dongfeng Road East, Guangzhou 510060, China. Email: qiubo@sysucc.org.cn; Hui Liu, MD, PhD. Department of Radiation Oncology, State Key Laboratory of Oncology in South China, Collaborative Innovation Center for Cancer Medicine, Guangdong Provincial Clinical Research Center for Cancer, Sun Yat-sen University Cancer Center, 651 Dongfeng Road East, Guangzhou 510060, China. Email: liuhuisysucc@126.com.

Background: Delineating gross tumor volume (GTV) using computed tomography (CT) imaging is the standard for lung cancer contouring, but discrepancies among observers compromise accuracy and reliability. Magnetic resonance imaging (MRI) provides superior soft-tissue resolution compared to CT, thus, we design this retrospective study to compare the treatment outcomes of magnetic resonance-based (MR-based) and CT-based tumor delineation in locally advanced non-small cell lung cancer (LA-NSCLC) patients treated with hypo-fractionated concurrent chemoradiotherapy (hypo-CCRT).

Methods: A total of 293 LA-NSCLC patients treated with hypo-CCRT from three trials between October 2015 and October 2020 were screened. Ninety patients with each MR-based delineation and CT-based delineation of the primary tumor were selected for analysis. In the MR-based delineation group, T1-enhanced MR images was rigidly registered with 10 respiratory phases of planning CT images, respectively. The primary tumors were contoured on each respiratory phase based on co-registered MRI. The locoregional progression-free survival (LPFS), progression-free survival (PFS), overall survival (OS) and toxicities in both groups were analyzed.

Results: The 2-year LPFS rate was 69.2% [95% confidence interval (CI): 59.6–80.2%] in the MR-based delineation group and 61.0% (95% CI: 50.9–73.0%) in the CT-based delineation group (P=0.37). There was no significant difference in median PFS (P=0.45) or OS (P=0.69) between the two groups. The MR-based delineation group had smaller planning target volume (186.1 *vs.* 315.3 cm^3, P<0.001), lower incidences of ≥G2 pneumonitis (10% *vs.* 24.4%, P=0.001) and ≥G3 esophagitis (2.2% *vs.* 15.6%, P<0.001). In evaluating the patterns of recurrence, in-field recurrences were the dominant type in both groups (21 out of 27 patients in MR-based delineation group, 24 out of 32 patients in CT-based delineation group).

^ ORCID: 0009-0008-1771-2991.

Conclusions: MR-based delineation in hypo-CCRT was feasible and achieved similar treatment efficacy to CT-based delineation. The use of MR imaging to reduce the target volume resulted in promising local control and lower incidence of radiation-induced toxicities.

Keywords: Locally advanced non-small cell lung cancer (LA-NSCLC); hypofractionated radiotherapy; magnetic resonance-based delineation (MR-based delineation); computed tomography-based delineation (CT-based delineation)

Submitted Apr 18, 2024. Accepted for publication Sep 25, 2024. Published online Nov 06, 2024.
doi: 10.21037/tlcr-24-341
View this article at: https://dx.doi.org/10.21037/tlcr-24-341

Introduction

Radiotherapy plays a pivotal role in the treatment of locally advanced non-small cell lung cancer (LA-NSCLC). Conformal radiotherapy technology has undergone significant improvements over the decades. In patients with locally advanced or recurrent NSCLC, hypo-fractionated radiotherapy has been proved to be safe and effective, achieved by tailoring the fractionated dose and escalating the total dose (1-3). Compared to conventional fractionation schemes of radiotherapy, the hypo-fractionated regimens enhance radiation-induced anti-tumor immune responses (4), providing a basis for the combination of hypo-fractionated therapy and immunotherapy. Precise target definition is crucial for hypo-fractionated radiotherapy as it can improve treatment outcomes and reduce radiation-related toxicities (5). Delineation of the gross tumor volume (GTV) based on computed tomography (CT) imaging can significantly vary among different observers, particularly in cases involving atelectasis and obstructive pneumonitis (6). The application of fluorodeoxyglucose positron emission tomography (FDG-PET) reduces observer variability and improves lesion boundary sensitivity and specificity compared to CT alone (7). However, FDG-PET is not specific to malignant tissues and can also detect tissues with high glucose metabolism, making it challenging to differentiate between inflammatory and malignant tissues.

With the technological advancements in magnetic resonance imaging (MRI), such as sequencing, acceleration methods, parallel imaging techniques, utilization of contrast media, post-processing software and ultrashort echo time (UTE), have made magnetic resonance (MR) imaging highly useful in routine clinical practice for pulmonary disease (8-10). Compared to thin-section CT, MRI with UTE technology can capture fine pulmonary structures and lymph nodes with minimum diameters of 4 millimeters to maximum diameters of 30 millimeters, offering a reliable tool for diagnosing lung diseases (11,12). Additionally, the Radiologic Diagnostic Oncology Group (RDOG) suggested that the accuracies between MRI and CT in tumor assessment were comparable (13). When combined with diffusion-weighted sequence (DW-MRI), MRI has demonstrated diagnostic efficacy comparable to FDG-PET-CT in the staging of primary tumors and lymph nodes (14). But MRI provides superior soft-tissue resolution compared to CT, mainly in cases where tumors invade the chest wall, mediastinum, vascular and neural structures, or are

Highlight box

Key findings

- This study finds that magnetic resonance (MR)-based tumor delineation for hypo-fractionated concurrent chemoradiotherapy (CCRT) in locally advanced non-small cell lung cancer (LA-NSCLC) achieves comparable outcomes in local control and survival compared to computed tomography (CT)-based delineation CCRT. Meanwhile, lower incidence of radiation-induced toxicities observed in patients with MR-based tumor delineation due to the smaller volumes of gross tumor volume (GTV).

What is known and what is new?

- The delineation of GTV based on CT imaging remains the mainstream approach to lung cancer contouring.
- Several studies have demonstrated the feasibility and advantages of using magnetic resonance imaging (MRI) for delineating lung tumor volumes. But there is limited evidence on comparing MRI-based delineation with CT-based delineation.

What is the implication, and what should change now?

- MR-based tumor delineation can be considered for radical-intent radiotherapy in LA-NSCLC to reduce treatment-related toxicity without compromising efficacy.

associated with atelectasis (13,15,16). Moreover, MRI has potential applications in various fields of radiotherapy, such as patient selection, tumors and organs at risk (OARs) delineation, image-based adaptive treatment delivery, and assessing treatment response (17,18). Several studies have now shown us the feasibility and benefits of using MRI to delineate the volume of lung tumors (19-21).

As MR-based radiation treatment planning is still a relatively new technology, further exploration in the areas of radiomics and focal boost may expand the boundaries of cancer diagnosis and treatment, leading to higher customization of cancer therapies. We have implemented MR into routine practice for better tumor delineation these years. Given that, we aimed to compare the treatment efficacy and toxicities of MR-based and CT-based tumor delineation in LA-NSCLC patients treated by hypo-fractionated concurrent chemoradiotherapy (hypo-CCRT). We present this article in accordance with the STROBE reporting checklist (available at https://tlcr.amegroups.com/article/view/10.21037/tlcr-24-341/rc).

Methods

Patient enrollment

Two hundred and thirty-three unresectable stage III NSCLC patients were selected from 3 prospective clinical trials conducted at Sun Yat-sen University Cancer Center between October 2015 and October 2020 (3,22,23). The involving studies were all approved by the institutional review boards of Guangdong Association Study of Thoracic Oncology (GASTO) and Sun Yat-sen University Cancer Center (approval numbers from GASTO: A2015-004, A2018-009, A2019-003; approval numbers from Sun Yat-sen University Cancer Center: B2015-041-01, B2018-029-01, B2019-075-01) and conducted according to the Declaration of Helsinki (as revised in 2013). All participants provided written informed consent. The ClinicalTrials.gov identifiers for the aforementioned trials are NCT02573506, NCT03659578 and NCT03900117, respectively. The protocol IDs for these studies are GASTO1011, GASTO1043 and GASTO1049, respectively.

Inclusion criteria were as follows: (I) histologically or cytologically confirmed unresectable stage IIIA–C NSCLC; (II) an Eastern Cooperative Oncology Group (ECOG) performance status score of 0 to 2; (III) received hypo-fractionated radiotherapy with concurrent chemotherapy; (IV) underwent chest MRI within two weeks prior to hypo-CCRT. Patients with a history of other cancers or previous thoracic radiotherapy were excluded. After screening, a total of 216 patients were eligible for this study, including 98 patients with MR-based delineation and 118 patients with CT-based delineation. To control for potential confounder, a 1:1 propensity score matching was performed among the 216 patients based on tumor-node-metastasis (TNM) stage (including stage IIIA *vs.* IIIB *vs.* IIIC), ECOG score and age. Finally, 180 patients were included in this study, including 90 in MR-based delineation group and 90 in CT-based delineation group.

4D-CT simulation and MRI sequence

All patients received 4D-CT simulation scan using the Brilliance Big Bore scanner from the atlas to the second lumbar vertebra with a slice thickness of 3 mm. The Real-time Position Management system respiratory gating hardware (Varian Medical Systems, Palo Alto, CA, USA) was used to record the patient's breathing pattern during the CT scan. For 4D-CT images, the respiratory signal data was reconstructed and divided into 10 equally spaced time percentage bins (from 0% to 90% maximum inhalation), with each bin representing 10% of the respiratory cycle. Thus, the 0% breathing phase corresponds to the peak of inhalation, and the 50% breathing phase corresponds to the peak of exhalation. The 20% breathing phase image was close to mid-ventilation, so for clinical convenience, we chose this phase to formulate treatment planning (24,25). Patients were immobilized in the same treatment position for both MRI and planning CT acquisition. MRI was acquired at two 1.5 T magnetic scanners (Signal HDx 1.5 T, GE Medical System, Milwaukee, Wisconsin, USA; Magnetom Aera 1.5 T, Siemens, Shenzhen, China) and one 3.0 T magnetic scanner (Discovery MR750w 3.0 T, GE Medical System, Milwaukee, Wisconsin, USA) with a slice thickness of 3 mm. The contrast-enhanced T1-weighted (T1C) sequence was chosen as the MR sequence to register with each respiratory phase, centered on the primary tumor. To suppress the fatty tissue signal, we utilized the "water only" image contrast (26).

Region of interest (ROI) delineation

The GTV was defined as the visual primary tumor (GTVp) and the locoregional metastatic lymph nodes (GTVn). For the MR-based delineation group, we first performed rigid registration of the primary tumor between the T1-

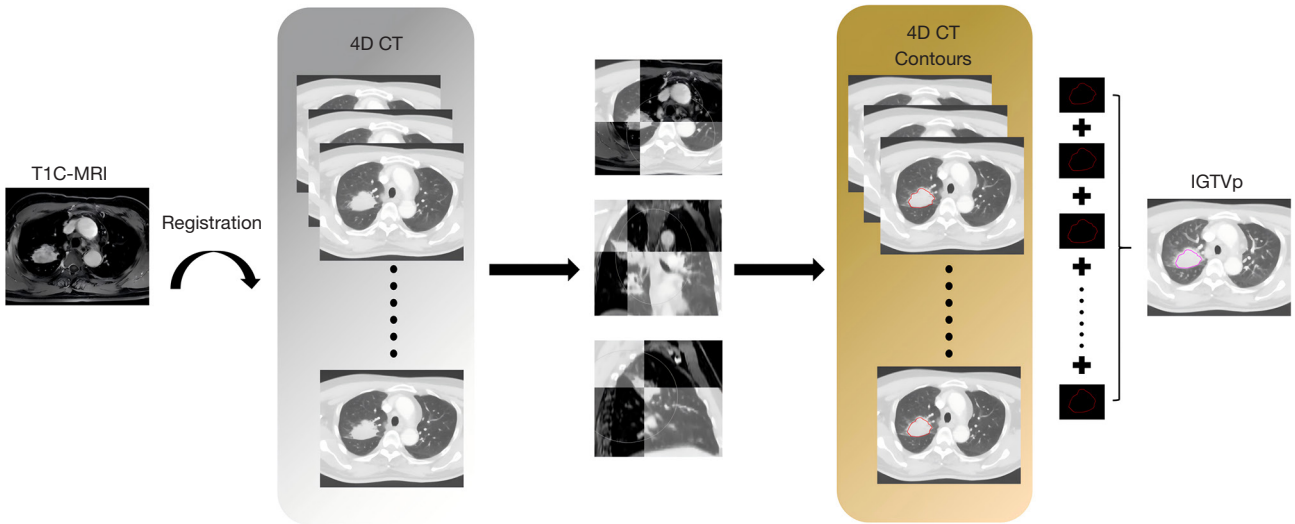

Figure 1 Schematic illustration of image registration and primary tumor contour using T1C-MR images. This approach consisted of three steps: (I) MRI and planning CT registration; (II) manual adjustments in coronal, sagittal and transverse planes; (III) summarizing the GTVp from 10 respiratory phases to form the IGTV. The red-encircled areas represent the GTVps delineated across 10 respiratory phases. The purple-encircled area represents the IGTVp, which is composed of GTVps from 10 respiratory phases. T1C-MRI, contrast-enhanced T1-weighted sequence magnetic resonance image; 4D-CT, four-dimensional computed tomography; IGTVp, internal primary gross tumor volume; MRI, magnetic resonance image; CT, computed tomography; GTVp, primary gross tumor volume; IGTV, internal gross tumor volume.

enhanced MR images and the lung window CT images (width/level, 1,600/–600 HU) for each of the 10 respiratory phases respectively. The registration was conducted using mutual information-based matching and was then manually reviewed to ensure the quality of the registration. Following this, on each respiratory phase of the CT, the GTVp from the MR images was propagated according to the transformation. The results were visually verified, and necessary modifications were made. Finally, the GTVps from the 10 respiratory phases were merged to form the internal GTVp (IGTVp). The internal GTVn (IGTVn) was generated based on the mediastinal window CT images (width/level, 400/20 HU) (*Figure 1*). As for the CT-based delineation group, GTVp and GTVn were separately contoured on each 10 respiratory phases of lung window and mediastinal window CT images. In both groups, an internal GTV (IGTV) was obtained by summing the GTVs from 10 respiratory motion phases. Then, a 5 mm margin is added to the IGTV to account for setup uncertainties, resulting in the planning tumor volume (PTV). Of note, for patients with atelectasis who did not underwent PET-CT, we typically delineated tumor boundaries on CT images by adjusting the window width and level, while using MRI as a reference to define the boundaries and finalize the contours in consultation with experienced radiologists. OARs, including lungs, spinal cord and heart were contoured on the 20% breathing phase of planning CT for dose constraint evaluation. All delineations of OARs adhere to the European Society for Radiotherapy & Oncology (ESTRO) ACROP guidelines (27), except for esophagus in the MR-based delineation group, where delineation was carried out on the mediastinal window CT based on MRI.

CCRT

Patients involved in the study underwent concurrent chemotherapy and hypo-fractionated radiotherapy with the technique of intensity-modulated radiation therapy/volumetric modulated arc therapy (IMRT/VMAT) using conventional linacs. The median dose of hypo-fractionated radiotherapy and boost was 64 Gy (range, 54–68 Gy, 4 or 5 Gy per fraction) for the MR-based delineation group and 68 Gy (range, 64–75 Gy, 3 or 4 Gy per fraction) for the CT-based delineation group. Daily cone beam CT (CBCT) was used for guidance during radiotherapy delivery. Each patient received a weekly concurrent chemotherapy regimen, which

included docetaxel (25 mg/m^2) and nedaplatin (25 mg/m^2).

Definition of local failure

Locoregional recurrence was defined as the re-emergence of a malignancy at the primary site of the original tumor or within the adjacent lymph nodes. CT imaging performed at the time of locoregional recurrence was registered to the original simulation CT using Zeus Cloud TPS software V1.0 (Tongdiao, Suzhou, China). Bone landmarks were used for rigid registration, which was followed by visual correction relying on soft tissue structures. All measurable anatomic regions of recurrent GTVs (rGTVs) were contoured by an experienced radiation oncologist in thoracic service. The rGTVs were then mapped to the original IGTVs from the original treatment planning. The rGTVs were classified as follows: (I) in-field recurrence (95% of rGTV was located within the 95% isodose); (II) marginal recurrence (20–95% of rGTV was located within the 95% isodose); (III) out-of-field recurrence (less than 20% of rGTV was located within the 95% isodose) (28).

Follow-up

For the first 2 years following treatment, chest and upper abdomen CT scans were conducted every 3 months, and then every 6 months for the third to fifth years. Furthermore, during the first 5 years, brain MRI scans were conducted every 6 months. PET-CT scans and biopsies were recommended if there was suspected locoregional or distant disease progression. Treatment responses were first evaluated by an independent radiation oncologist and confirmed by a senior physician eight weeks after completion of hypo-CCRT using Response Evaluation Criteria in Solid Tumors version 1.1. Therapeutic toxicities were graded and recorded based on the Common Terminology Criteria (CTC) for Adverse Events version 5.0.

Statistical analysis

The locoregional progression-free survival (LPFS) was defined as the time from the initiation of radiotherapy to disease progression in primary tumor site or regional lymph nodes. The progression-free survival (PFS), defined as the time from radiotherapy to death or disease progression; overall survival (OS), defined as the time from radiotherapy to death from any cause.

Treatment-related toxicities were classified according to CTC version 5.

Survival curves were plotted using the Kaplan-Meier method and compared using the log-rank test. The distribution of patient characteristics between groups was compared using Wilcoxon rank sum test or Chi-squared tests. The Wilcoxon rank sum test was used to compare dosimetric parameters and toxicities between two groups. Statistical analysis was conducted using SPSS 23 software (IBM, Chicago, IL, USA), with a two-sided P value <0.05 considered statistically significant.

Results

Clinical characteristics

The clinical characteristics of the 180 eligible patients were summarized in *Table 1*. The median age for the MR-based and CT-based delineation groups was 59 (range, 28–89) and 58.5 (range, 28–77) years, respectively. There were no significant differences in age, ECOG score, and disease stage distribution (including T stage, N stage and M stage) between the two groups. Squamous cell carcinoma accounted for more than half of the cases in both groups: 60.0% (54/90) in the MR-based delineation group and 53.3% (48/90) in the CT-based delineation group. The tumor locations and treatment modalities were comparable between the two groups.

Local control and survival

The median follow-up duration for the whole cohort was 36.3 months [95% confidence interval (CI): 31.1–41.5], with a median follow-up time of 29.7 months (95% CI: 29.2–30.2) for the MR-based delineation group and 44.3 months (95% CI: 39.4–47.1) for the CT-based delineation group. The 1- and 2-year LPFS rates for the MR-based delineation group were 80.3% (95% CI: 72.4–89.2%) and 69.2% (95% CI: 59.6–80.2%), which were similar to the CT-based delineation group, which were 76.4% (95% CI: 67.9–86.0%) and 61.0% (95% CI: 50.9–73.0%), respectively (P=0.37, *Figure 2A*). The median OS durations were 28.4 months (95% CI: 22.2–34.6) in the MR-based delineation group compared with 27.0 months (95% CI: 19.7–34.3) in the CT-based delineation group (P=0.69, *Figure 2B*). The median PFS were 12.9 months (95% CI: 11.6–14.2) in the MR-based delineation group compared with 12.1 months (95% CI: 10.5–13.7) in the CT-based delineation group (P=0.45, *Figure 2C*). The 2-year distant metastasis-free survival (DMFS) was not

Table 1 Clinical characteristics in the MR-based and CT-based delineation groups

Patient characteristics	MR-based delineation group (n=90)	CT-based delineation group (n=90)	Test
Age (years), median [range]	59 [28–89]	58.5 [28–77]	χ^2, P=0.39
Gender, n (%)			Wilcoxon, P=0.27
Male	74 (82.2)	68 (75.6)	
Female	16 (17.8)	22 (24.4)	
ECOG PS, n (%)			Wilcoxon, P=0.54
0	29 (32.2)	35 (38.9)	
1	61 (67.8)	52 (57.8)	
2	0	3 (3.3)	
Disease stage, n (%)			Wilcoxon, P=0.17
IIIA	23 (25.6)	30 (33.3)	
IIIB	34 (37.8)	39 (43.3)	
IIIC	33 (36.7)	21 (23.3)	
T stage, n (%)			Wilcoxon, P=0.21
1	7 (7.8)	8 (8.9)	
2	20 (22.2)	25 (27.8)	
3	31 (34.4)	33 (36.7)	
4	32 (35.6)	24 (26.7)	
N stage, n (%)			Wilcoxon, P=0.85
0	2 (2.2)	2 (2.2)	
1	9 (10.0)	10 (11.1)	
2	36 (40.0)	36 (40.0)	
3	43 (47.8)	42 (46.7)	
Histologic classification, n (%)			Wilcoxon, P=0.63
Squamous cell carcinoma	54 (60.0)	48 (53.3)	
Adenocarcinoma	20 (22.2)	30 (33.3)	
Other subtypes	16 (17.8)	12 (13.3)	
Tumor location, n (%)			Wilcoxon, P=0.88
Central	57 (63.3)	56 (62.2)	
Peripheral	33 (36.7)	34 (37.8)	
Treatment, n (%)			Wilcoxon, P=0.07
Neoadjuvant treatment followed by CCRT	80 (88.9)	70 (77.8)	
CCRT	10 (11.1)	20 (22.2)	

Chi-squared tests (χ^2) was used for the comparison of continuous variables between the two groups; Wilcoxon rank sum test was used for the comparison of categorical variables between the two groups. MR, magnetic resonance; CT, computed tomography; ECOG PS, Eastern Cooperative Oncology Group physical status; CCRT, concurrent chemoradiotherapy.

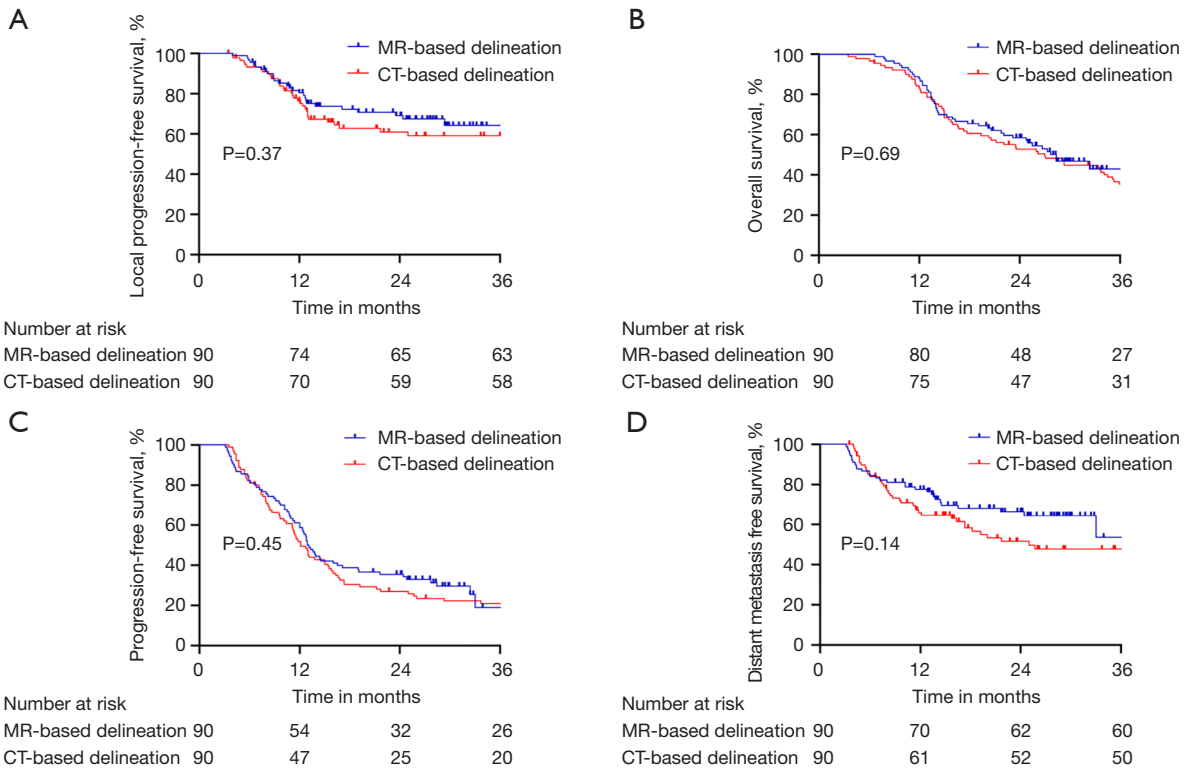

Figure 2 Kaplan-Meier plots and P values of (A) local progression-free survival, (B) overall survival, (C) progression-free survival and (D) distant metastasis free survival in the two groups. MR, magnetic resonance; CT, computed tomography.

significantly different between the two groups, with rates of 66.4% (95% CI: 56.8–77.6%) in the MR-based delineation group and 51.8% (95% CI: 41.6–64.7%) in the CT-based delineation group (P=0.14, *Figure 2D*).

Radiation dose distribution of tumors and OARs

Dosimetric data and target volumes for both MR-based and CT-based delineation groups are presented in *Table 2*. The mean total dose was 63.6 Gy in the MR-based delineation group and 68.3 Gy in the CT-based delineation group, respectively. Although the MR-based delineation group had a smaller median IGTV (78.2 cm^3) than the CT-based group (86.7 cm^3), there was no significant difference in median IGTV between the two groups (P=0.37). As for the median PTV, the MR-based delineation group (186.1 cm^3) was significantly smaller than the CT-based delineation group (315.3 cm^3, P<0.001). The MR-based delineation group had a lower mean lung dose (median, 13.9 *vs.* 20.0 Gy; P<0.001), and a lower lung V20 (bilateral, ipsilateral, and contralateral lung) than the CT-based delineation group. The MR-based delineation group had lower V40 and V50 of the esophagus (28.7% and 6.3%, respectively) than the CT-based delineation group (55.2% and 27.8%, respectively) (P<0.001). Additionally, the MR-based delineation group had lower V25 (8.3% *vs.* 14.3%, P=0.004) and V30 of the heart (5.3% *vs.* 11.0%, P=0.01) compared to the CT-based delineation group.

The dose-volume histogram (DVH) and dose distribution for one same patient under the MR-based and CT-based delineation are shown in *Figure 3*. The MR-based delineation treatment plan exhibits smaller IGTV (circled in red) and PTV (circled in blue) boundaries than the CT-based counterpart. In the MR-based delineation treatment plan, the prescription dose delivered to 100% volume of the PTV, V20 of bilateral lungs and V40 of the esophagus were 90.78%, 26.49%, and 14.61%, respectively. In the CT-based delineation treatment plan, the prescription dose delivered to 100% of the PTV, V20 of bilateral lungs and V40 of esophagus were 91.5%, 30.38%, and 17.17%, respectively.

Table 2 Dosimetric parameters of tumors and OARs in the two groups

Dosimetric factors	MR-based delineation group (n=90)		CT-based delineation group (n=90)		P
	Median	Q1–Q3	Median	Q1–Q3	
IGTV volume, cm^3	78.2	55.1–121.8	86.7	59.3–117.6	0.37
PTV volume, cm^3	186.1	126.3–264.9	315.3	212.9–429.7	<0.001
Median dose to IGTV, Gy	67.2	66.5–67.7	71.7	71.2–72.3	<0.001
Median dose to PTV, Gy	65.6	64.5–66.3	70.5	69.6–71.2	<0.001
Median D95% of PTV, Gy	61.2	60.2–61.9	64.8	63.7–65.5	<0.001
Lungs					
Median lung dose, Gy	13.9	7.7–19.1	20.0	14.8–24.4	<0.001
V20 of bilateral lungs, %	23.5	20.3–26.4	37.2	31.8–38.7	<0.001
V20 of ipsilateral lung, %	37.1	32.6–44.3	56.2	52.1–63.3	<0.001
V20 of contralateral lung, %	9.7	5.7–13.0	15.7	11.7–20.1	<0.001
Esophagus					
Max dose of esophagus, Gy	59.1	54.9–62.9	64.2	61.8–66.7	<0.001
V40, %	28.7	15.6–40.7	55.2	49.2–62.6	<0.001
V50, %	6.3	0.6–12.9	27.8	17.3–40.9	<0.001
Heart					
Max dose of heart, Gy	67.5	62.9–68.9	70.2	65.5–73.4	<0.001
V25, %	8.3	3.2–16.3	14.3	9.8–25.4	0.004
V30, %	5.3	2.0–11.2	11.0	7.1–18.9	0.01

OAR, organ at risk; MR, magnetic resonance; CT, computed tomography; IGTV, internal gross tumor volume; PTV, planning target volume; D95%, the minimum coverage dose of 95% of the target.

Toxicity

Safety analyses were performed for both groups, and the results are presented in *Table 3*. No grade (G) 5 toxicity events occurred in either group. Patients in the MR-based delineation group had a lower incidence of radiation-induced pneumonitis, esophagitis, thrombocytopenia, and lymphocytopenia compared to those in the CT-based delineation group. The incidence of G2 or higher pneumonitis was significantly lower in the MR-based delineation group (10%; 9/90) compared to the CT-based delineation group (24.4%; 22/90) (P=0.001). The incidence of G3 or higher esophagitis was significantly lower in the MR-based delineation group (2.2%, 2/90) than in the CT-based delineation group (15.6%, 14/90, P<0.001). As for hematologic toxicities, no G2 or higher thrombocytopenia was observed in the MR-based delineation group, while eight (8.9%, 8/90) occurred in the CT-based delineation group (P=0.01). The incidence of G3–4 lymphocytopenia was lower in the MR-based delineation group (36.7%; 33/90) than in the CT-based delineation group (72.2%; 65/90) (P<0.001).

Tumor response to hypo-CCRT

The objective response rates (ORRs) of hypo-CCRT were evaluated 8 weeks after the completion of the treatment (Table S1). The short-term responses were similar between the two groups (P=0.79), with objective response [complete response + partial response (CR + PR)] rates of 82.2% in

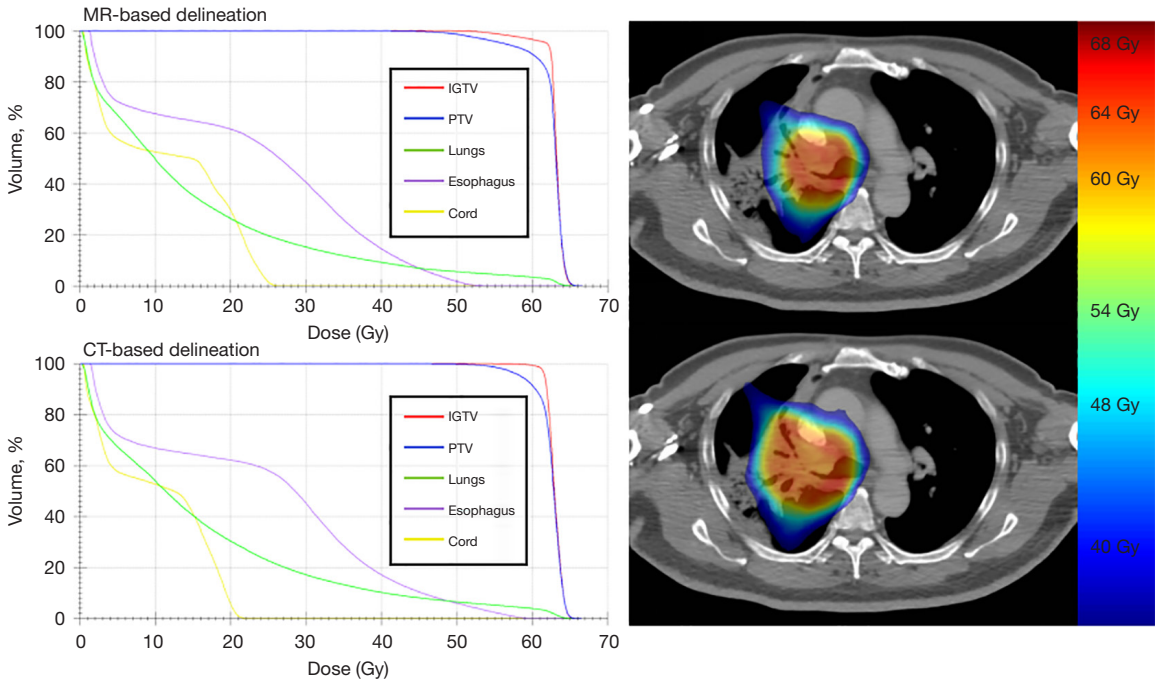

Figure 3 Exemplary of cumulative DVH and dose distribution in one same patient under MR-based delineation treatment plan and CT-based delineation treatment plan. MR, magnetic resonance; CT, computed tomography; IGTV, internal gross tumor volume; PTV, planning target volume; DVH, dose-volume histogram.

Table 3 Incidence of treatment-related toxicities

Events	MR-based delineation group (n=90), n (%)					CT-based delineation group (n=90), n (%)					P value
	Grade 0	Grade 1	Grade 2	Grade 3	Grade 4	Grade 0	Grade 1	Grade 2	Grade 3	Grade 4	
Pneumonitis	19 (21.1)	62 (68.9)	9 (10.0)	0	0	7 (7.8)	61 (67.8)	18 (20.0)	4 (4.4)	0	0.001
Esophagitis	46 (51.1)	19 (21.1)	23 (25.6)	2 (2.2)	0	15 (16.7)	19 (21.1)	42 (46.7)	14 (15.6)	0	<0.001
Aleucocytosis	48 (53.3)	20 (22.2)	19 (21.1)	3 (3.3)	0	42 (46.7)	24 (26.7)	20 (22.2)	4 (4.4)	0	0.43
Neutropenia	62 (68.9)	13 (14.4)	13 (14.4)	1 (1.1)	1 (1.1)	58 (64.4)	17 (18.9)	13 (14.4)	2 (2.2)	0	0.61
Anemia	38 (42.2)	41 (45.6)	10 (11.1)	1 (1.1)	0	42 (46.7)	39 (43.3)	7 (7.8)	2 (2.2)	0	0.52
Thrombocytopenia	83 (92.2)	7 (7.8)	0	0	0	72 (80.0)	10 (11.1)	3 (3.3)	5 (5.6)	0	0.01
Lymphocytopenia	4 (4.4)	20 (22.2)	33 (36.7)	29 (32.2)	4 (4.4)	1 (1.1)	3 (3.3)	21 (23.3)	51 (56.7)	14 (15.6)	<0.001

MR, magnetic resonance; CT, computed tomography.

both groups. Three (3.3%) in the MR-based delineation group and one (1.1%) in the CT-based delineation group had a CR, while 71 (78.9%) in the MR-based delineation group and 73 (81.1%) in the CT-based delineation group achieved a PR.

A patient who was assessed as PR by using both CT and MRI scans 2 months after the completion of hypo-CCRT was shown in Figure S1. Six months after the completion of hypo-CCRT, the residual lesion observed on the CT images was larger than that seen on the CT images taken 2 months after the completion of hypo-CCRT. In contrast, the MR imaging showed a continuous decrease in the size of the residual disease. Based on the radiological evidence from MR imaging, we considered that the patient achieved PR after hypo-CCRT, while the residual lesion observed on the CT scan was composed of atelectasis components.

Failure patterns

The disease progression patterns were presented in Table S2. There were 27 patients (30.0%, 27/90) in the MR-based delineation group and 32 patients (35.6%, 32/90) in the CT-based delineation group had locoregional progression. In the MR-based delineation group, in-field local recurrences occurred in 21 out of 27 patients (77.8%, 21/27), while in the CT-based delineation group, this was observed in 24 out of 32 patients (75.0%, 24/32). Marginal recurrences were observed in 5 patients (18.5%, 5/27) in the MR-based delineation group and 6 patients (18.8%, 6/32) in the CT-based delineation group. Only one patient (3.7%, 1/27) in the MR-based delineation group had out-of-field recurrence. Two patients (6.2%, 2/32) in the CT-based delineation group experienced co-existing in-field and out-field local recurrences during follow-up (both patients exhibited enlarged regional lymph nodes and in-field recurrent lesions). Distant metastases were identified in 30 patients (33.3%, 30/90) in the MR-based delineation group and 41 patients (45.6%, 41/90) in the CT-based delineation group. Five patients (5.6%, 5/90) in the MR-based delineation group and 20 patients (22.2%, 20/90) in the CT-based delineation group were identified concurrent locoregional failure and distant metastases.

Discussion

This present study results showed that LA-NSCLC patients who received hypo-CCRT with either MR- or CT-based delineation had comparable local control and survival rates. In addition, our data indicated that the reduction of volumes informed by MRI resulted in lower incidence of radiation-induced toxicities, and does not confer an increased risk of out-of-field progression.

CT imaging has limitations in accurately delineating tumor boundaries due to its limited soft tissue resolution. As a result, it might miss or exceed the true extent of the tumor. In contrast, MRI is effective in assessing atelectasis, mediastinal and chest wall invasion. Our previous and current studies had demonstrated the efficacy of thoracic MRI in defining primary lung tumor boundaries (29). Compared to PET imaging, MRI offers superior spatial resolution for determining the tumor target. So far, there has been no consensus on which MRI sequence to choose for target delineation in lung cancer. Previous studies have recommended T2-weighted HASTE (21), contrast-enhanced T1-weighted (19), and diffusion-weighted imaging (DWI) (30) MRI sequences. Based on our experience, we chose the contrast-enhanced T1-weighted MRI sequence with fat suppression to delineate the boundaries of the primary tumor and regional lymph nodes, given its clarity in differentiating tumor edges from adjacent tissues.

This study found comparable local control in both groups. Well-defined tumor boundaries identified by MRI led to smaller IGTV and PTV. Although the MR-based delineation group had a reduced irradiation volume, most local recurrences persisted as in-field recurrence, with only three patients experiencing out-field recurrence. Before the PACIFIC trial, nearly one-third of patients experienced local-regional relapse within one year (31,32). Patients in our study achieved a satisfactory 1-year LPFS (81.6% in MR-based delineation group), which was similar to the rate from patients treated with chemoradiotherapy followed by durvalumab (82–86%) (33,34). Therefore, enhancing local-regional control through CCRT continued to be promising for unresectable LA-NSCLC patients during the immunotherapy era. Integrating MR imaging and 4D-CT simulation for target delineation could serve as a novel image-based option for LA-NSCLC patients undergoing hypo-CCRT.

A diagnostic whole-body FDG-PET-CT is considered essential for precise tumor volume delineation in patients with LA-NSCLC according to ESTRO/ACROP guidelines. However, in China, financial constraints related to PET-CT present a challenge, as it is relatively expensive and not covered by medical insurance. On the other hand, MRI is included in the scope of insurance reimbursement, making it a more accessible option for patients. Consequently, in our routine clinical practice, while we highly recommend a pre-treatment PET-CT scan, it is not mandatory. Instead, chest MRI is conducted routinely due to its critical role in tumor delineation and response assessment, as supported by previous studies (14,20,35). In our study, 45 patients (25%) underwent PET-CT before treatment, with 21 in the MR-based delineation group and 24 in the CT-based delineation group. The remaining 135 patients (75%) who did not undergo PET-CT were evaluated using enhanced chest and abdominal CT, brain MRI, and whole-body bone scans for staging. Additionally, all patients in both groups underwent chest MRI. Thus, while the absence of PET-CT in most patients introduces a potential risk of stage migration, this risk is comparable across both groups. The slight, statistically insignificant, difference in DMFS between the MR-based and CT-based delineation groups

might be attributed to the shorter follow-up duration in the MR-based delineation group, leading to a lack of endpoint events by the end of the follow-up period.

Patients with MR-based delineation were associated with a reduced incidence of treatment-related toxicities, which may be attributed to the superior soft-tissue contrast allowing for precise delineation of OARs and target volumes. Our previous study suggested that the esophagus-sparing technique reduces radiation-induced esophagitis, improves nutrition status, and lowers the grade of radiation-induced pneumonitis (36). The precise delineation of the esophagus using MR imaging in this study resulted in a nearly 50% reduction in the incidence of grade ≥2 esophagitis compared to the CT-based delineation group. Previous findings demonstrated increased irradiation volumes to pulmonary tumors could cause not only direct injury to the lungs but also severe lymphopenia (37). Our data illustrated MR-based delineation led to significantly lower doses to the lobes, resulting in a lower incidence of radiation-induced pneumonitis and lymphopenia. The significant reduction in pneumonitis and lymphopenia rates achieved through MR-based delineation lends strong support to the combination of radiotherapy and immunotherapy.

Certain limitations and biases remain in this study. First, all observers in this study were from the same center, and the use of contouring guidelines and a radiologist-led workshop further restricts the generalizability of the results. Nevertheless, these guidelines could help with the clinical application of MRI in GTV delineation for lung cancer radiotherapy. Second, the use of a flat top bed and curved MRI bed may have caused errors in image registration, and the respiratory motion was found to be the primary source of mis-registration, which could have affected the data analysis. Developing 4D-MRI for radiotherapy is still a challenge, but it has the potential to provide high-resolution information for creating motion-managed treatment plans, such as using an internal target volume or mid-position approach. Third, this study was retrospective and propensity-matched, so a larger randomized cohort might be necessary to validate the results. Finally, real-time MR imaging and adaptive planning during radiotherapy were not used in this study but could be explored in future research.

Conclusions

The use of MR-based delineation hypo-CCRT was feasible and showed comparable rates of local control and survival when compared to CT-based delineation hypo-CCRT. The use of MR imaging to reduce the target volume resulted in lower incidence of radiation-induced toxicities without compromising local control. Further prospective studies are warranted to verify the present findings and to evaluate the prognostic potential of MR-based delineation for thoracic radiotherapy in clinical practice.

Acknowledgments

Funding: None.

Footnote

Reporting Checklist: The authors have completed the STROBE reporting checklist. Available at https://tlcr.amegroups.com/article/view/10.21037/tlcr-24-341/rc

Data Sharing Statement: Available at https://tlcr.amegroups.com/article/view/10.21037/tlcr-24-341/dss

Peer Review File: Available at https://tlcr.amegroups.com/article/view/10.21037/tlcr-24-341/prf

Conflicts of Interest: All authors have completed the ICMJE uniform disclosure form (available at https://tlcr.amegroups.com/article/view/10.21037/tlcr-24-341/coif). The authors have no conflicts of interest to declare.

Ethical Statement: The authors are accountable for all aspects of the work in ensuring that questions related to the accuracy or integrity of any part of the work are appropriately investigated and resolved. The involving studies were all approved by the institutional review boards of Guangdong Association Study of Thoracic Oncology (GASTO) and Sun Yat-sen University Cancer Center (approval numbers from GASTO: A2015-004, A2018-009, A2019-003; approval numbers from Sun Yat-sen University Cancer Center: B2015-041-01, B2018-029-01, B2019-075-01) and conducted according to the Declaration of Helsinki (as revised in 2013). All participants provided written informed consent.

References

1. Kong C, Zhu X, Shi M, et al. Survival and Toxicity of Hypofractionated Intensity Modulated Radiation Therapy in 4 Gy Fractions for Unresectable Stage III Non-Small Cell Lung Cancer. Int J Radiat Oncol Biol Phys 2020;107:710-9.
2. Chen N, Li Q, Wang S, et al. Hypo-fractionated radiotherapy with concurrent chemotherapy for locoregional recurrence of non-small cell lung cancer after complete resection: A prospective, single-arm, phase II study (GASTO-1017). Lung Cancer 2021;156:82-90.
3. Qiu B, Xiong M, Luo Y, et al. Hypofractionated Intensity Modulated Radiation Therapy With Concurrent Chemotherapy in Locally Advanced Non-Small Cell Lung Cancer: A Phase II Prospective Clinical Trial (GASTO1011). Pract Radiat Oncol 2021;11:374-83.
4. Siva S, MacManus MP, Martin RF, et al. Abscopal effects of radiation therapy: a clinical review for the radiobiologist. Cancer Lett 2015;356:82-90.
5. Njeh CF. Tumor delineation: The weakest link in the search for accuracy in radiotherapy. J Med Phys 2008;33:136-40.
6. Van de Steene J, Linthout N, de Mey J, et al. Definition of gross tumor volume in lung cancer: inter-observer variability. Radiother Oncol 2002;62:37-49.
7. Fox J, Ford E, Redmond K, et al. Quantification of tumor volume changes during radiotherapy for non-small-cell lung cancer. Int J Radiat Oncol Biol Phys 2009;74:341-8.
8. Koyama H, Ohno Y, Seki S, et al. Magnetic resonance imaging for lung cancer. J Thorac Imaging 2013;28:138-50.
9. Ohno Y. New applications of magnetic resonance imaging for thoracic oncology. Semin Respir Crit Care Med 2014;35:27-40.
10. Ciliberto M, Kishida Y, Seki S, et al. Update of MR Imaging for Evaluation of Lung Cancer. Radiol Clin North Am 2018;56:437-69.
11. Ohno Y, Koyama H, Yoshikawa T, et al. Pulmonary high-resolution ultrashort TE MR imaging: Comparison with thin-section standard- and low-dose computed tomography for the assessment of pulmonary parenchyma diseases. J Magn Reson Imaging 2016;43:512-32.
12. Ohno Y, Koyama H, Yoshikawa T, et al. Standard-, Reduced-, and No-Dose Thin-Section Radiologic Examinations: Comparison of Capability for Nodule Detection and Nodule Type Assessment in Patients Suspected of Having Pulmonary Nodules. Radiology 2017;284:562-73.
13. Webb WR, Gatsonis C, Zerhouni EA, et al. CT and MR imaging in staging non-small cell bronchogenic carcinoma: report of the Radiologic Diagnostic Oncology Group. Radiology 1991;178:705-13.
14. Fleckenstein J, Jelden M, Kremp S, et al. The Impact of Diffusion-Weighted MRI on the Definition of Gross Tumor Volume in Radiotherapy of Non-Small-Cell Lung Cancer. PLoS One 2016;11:e0162816.
15. Khalil A, Majlath M, Gounant V, et al. Contribution of magnetic resonance imaging in lung cancer imaging. Diagn Interv Imaging 2016;97:991-1002.
16. Qi LP, Zhang XP, Tang L, et al. Using diffusion-weighted MR imaging for tumor detection in the collapsed lung: a preliminary study. Eur Radiol 2009;19:333-41.
17. Owrangi AM, Greer PB, Glide-Hurst CK. MRI-only treatment planning: benefits and challenges. Phys Med Biol 2018;63:05TR01.
18. Kashani R, Olsen JR. Magnetic Resonance Imaging for Target Delineation and Daily Treatment Modification. Semin Radiat Oncol 2018;28:178-84.
19. Zhang H, Fu C, Fan M, et al. Reduction of inter-observer variability using MRI and CT fusion in delineating of primary tumor for radiotherapy in lung cancer with atelectasis. Front Oncol 2022;12:841771.
20. Karki K, Saraiya S, Hugo GD, et al. Variabilities of Magnetic Resonance Imaging-, Computed Tomography-, and Positron Emission Tomography-Computed Tomography-Based Tumor and Lymph Node Delineations for Lung Cancer Radiation Therapy Planning. Int J Radiat Oncol Biol Phys 2017;99:80-9.
21. Kumar S, Holloway L, Boxer M, et al. Variability of gross tumour volume delineation: MRI and CT based tumour and lymph node delineation for lung radiotherapy. Radiother Oncol 2022;167:292-9.
22. Zhou R, Qiu B, Xiong M, et al. Hypofractionated Radiotherapy followed by Hypofractionated Boost with weekly concurrent chemotherapy for Unresectable Stage III Non-Small Cell Lung Cancer: Results of A Prospective Phase II Study (GASTO-1049). Int J Radiat Oncol Biol Phys 2023;117:387-99.
23. Liu F, Qiu B, Xi Y, et al. Efficacy of Thymosin α1 in Management of Radiation Pneumonitis in Patients With

Locally Advanced Non-Small Cell Lung Cancer Treated With Concurrent Chemoradiotherapy: A Phase 2 Clinical Trial (GASTO-1043). Int J Radiat Oncol Biol Phys 2022;114:433-43.
24. Khamfongkhruea C, Thongsawad S, Tannanonta C, et al. Comparison of CT images with average intensity projection, free breathing, and mid-ventilation for dose calculation in lung cancer. J Appl Clin Med Phys 2017;18:26-36.
25. Tascón-Vidarte JD, Stick LB, Josipovic M, et al. Accuracy and consistency of intensity-based deformable image registration in 4DCT for tumor motion estimation in liver radiotherapy planning. PLoS One 2022;17:e0271064.
26. Dixon WT. Simple proton spectroscopic imaging. Radiology 1984;153:189-94.
27. Nestle U, De Ruysscher D, Ricardi U, et al. ESTRO ACROP guidelines for target volume definition in the treatment of locally advanced non-small cell lung cancer. Radiother Oncol 2018;127:1-5.
28. Jouglar E, Isnardi V, Goulon D, et al. Patterns of locoregional failure in locally advanced non-small cell lung cancer treated with definitive conformal radiotherapy: Results from the Gating 2006 trial. Radiother Oncol 2018;126:291-9.
29. Wang D, Qiu B, He H, et al. Tumor response evaluation by combined modalities of chest magnetic resonance imaging and computed tomography in locally advanced non-small cell lung cancer after concurrent chemoradiotherapy. Radiother Oncol 2022;168:211-20.
30. Shen G, Hu S, Deng H, et al. Performance of DWI in the Nodal Characterization and Assessment of Lung Cancer: A Meta-Analysis. AJR Am J Roentgenol 2016;206:283-90.
31. Machtay M, Paulus R, Moughan J, et al. Defining local-regional control and its importance in locally advanced non-small cell lung carcinoma. J Thorac Oncol 2012;7:716-22.
32. Bradley JD, Paulus R, Komaki R, et al. Standard-dose versus high-dose conformal radiotherapy with concurrent and consolidation carboplatin plus paclitaxel with or without cetuximab for patients with stage IIIA or IIIB non-small-cell lung cancer (RTOG 0617): a randomised, two-by-two factorial phase 3 study. Lancet Oncol 2015;16:187-99.
33. Abe T, Saito S, Iino M, et al. Effect of durvalumab on local control after concurrent chemoradiotherapy for locally advanced non-small cell lung cancer in comparison with chemoradiotherapy alone. Thorac Cancer 2021;12:245-50.
34. Taugner J, Käsmann L, Eze C, et al. Durvalumab after Chemoradiotherapy for PD-L1 Expressing Inoperable Stage III NSCLC Leads to Significant Improvement of Local-Regional Control and Overall Survival in the Real-World Setting. Cancers (Basel) 2021;13:1613.
35. Basson L, Jarraya H, Escande A, et al. Chest Magnetic Resonance Imaging Decreases Inter-observer Variability of Gross Target Volume for Lung Tumors. Front Oncol 2019;9:690.
36. Ma L, Qiu B, Li Q, et al. An esophagus-sparing technique to limit radiation esophagitis in locally advanced non-small cell lung cancer treated by simultaneous integrated boost intensity-modulated radiotherapy and concurrent chemotherapy. Radiat Oncol 2018;13:130.
37. Abravan A, Faivre-Finn C, Kennedy J, et al. Radiotherapy-Related Lymphopenia Affects Overall Survival in Patients With Lung Cancer. J Thorac Oncol 2020;15:1624-35.

Cite this article as: Zhang P, Ding S, Peng K, He H, Wang D, Zhou R, Wang B, Guo J, Liu H, Huang X, Xie C, Liu H, Qiu B. Comparing the outcomes of MR-based versus CT-based tumor delineation in locally advanced non-small cell lung cancer treated with hypo-fractionated radiotherapy and concurrent chemotherapy. Transl Lung Cancer Res 2024;13(11):2890-2902. doi: 10.21037/tlcr-24-341